

Confined Neutrino Oscillation

Pralay Chakraborty*

Physics Department, Gauhati University, India

Subhankar Roy†

Physics Department, Gauhati University, India.

(Dated: May 16, 2022)

We set a thought experiment concerning the neutrino oscillation probability, by assuming neutrino to be confined within an impenetrable well. We adopt the Pontecorvo's approach and the neutrino oscillation is visualized with respect to time in both relativistic and non-relativistic regimes. We see that the oscillation frequency depends on the energy of the mass eigenstates. Apart from this, a contrasting result of non-zero oscillation probability is obtained even if the mass eigenstates are degenerate.

I. INTRODUCTION

The neutrinos belong to the lepton family and the idea was first introduced by Wolfgang Pauli in the year of 1930. The neutrinos, unlike the charged leptons, are electromagnetically neutral and participate only in the weak interaction processes. The Standard Model [1–3] of particle physics cannot explain the origin of neutrino mass. However, from quantum mechanics point of view, we understand that the neutrino flavor states ($\nu_{eL}, \nu_{\mu L}, \nu_{\tau L}$) are not the mass eigenstates. The three neutrino mass eigenstates (ν_1, ν_2, ν_3) have mass eigenvalues m_1, m_2 and m_3 . The flavor states of neutrino can be expressed as the linear superposition of the mass eigenstates (ν_1, ν_2, ν_3). This is called flavor mixing [4, 5] and it can be demonstrated as shown in the following,

$$\begin{bmatrix} \nu_{eL} \\ \nu_{\mu L} \\ \nu_{\tau L} \end{bmatrix} = U \begin{bmatrix} \nu_1 \\ \nu_2 \\ \nu_3 \end{bmatrix}. \quad (1)$$

where, U is known as Pontecorvo-Maki-Nakagawa-Sakata(PMNS) matrix. As the mass eigenstates evolve in time, an alteration in the neutrino flavors occurs as it travels from the source to the detector. This phenomenon is called neutrino oscillation [6–8] and it was first introduced by Bruno Pontecorvo in 1957. If an electron type neutrino ν_e travels from source to detector, the probability that the detector will record the flavor as ν_μ is given as,

$$P_{\nu_e \rightarrow \nu_\mu} = \sin^2(2\theta) \sin^2 \left(\frac{\Delta m_{21}^2 c^3 l}{4E\hbar} \right), \quad (2)$$

where, $\Delta m_{21}^2 = m_2^2 - m_1^2$, l is the oscillation length and E stands for the energy of the neutrinos. The angle θ

is a parameter that signifies the mixing among the states ν_1 and ν_2 . It is worth noting that Pontecorvo assumed the neutrinos to be ultra-relativistic and carrying equal momenta. It is evident from Eq. (2) that if the neutrino oscillation has to occur, the mass eigenstates must be non-degenerate.

We know that neutrinos hardly interact with matter. So, we hypothesize some interaction to which neutrinos may respond strongly and consider a thought experiment where neutrino is trapped inside an infinite square well potential. We know that when a particle is trapped inside a potential well, the former may be in any one of the quantized energy states depicted by the quantum number n . In this regard, we expect that the oscillation probability will depend on the quantum number of the corresponding mass eigenstates. Keeping aside the fact that the neutrinos are spin half particles, we employ the Schrödinger equation and Klein-Gordon equation to study the neutrino oscillation in non-relativistic and relativistic scenarios respectively. Similarly, if we consider the spin half nature of the neutrino, the neutrino oscillation can be studied in the light of Dirac and Majorana equations. We study the oscillation probability for both two and three flavor cases. We know that confining a relativistic particle in a square well potential and allowing the potential height to go to infinity is not that straightforward. Because, this would lead to the Klein Paradox [9–13]. Precisely, the reflected flux from the wall is greater than the incident flux. However, we may avoid this problem and rescue the one-particle picture by considering a Lorentz scalar potential as the well height goes to infinity [14, 15]. We highlight that we express the oscillation probability with respect to time in the present work.

The plan of the paper is given as follows: In section II, we give the parametrization of the PMNS matrix and the numerical values of the required parameters for our work. We study the neutrino oscillation probability inside an infinite square well potential in section III. In section IV, we compare the oscillation frequency for relativistic and non-relativistic scenarios. We give the conditions for no flavor oscillation in section V. We write the summary and discussion of our work in section VI.

* pralay@gauhati.ac.in

† subhankar@gauhati.ac.in

Parameters	$bt\bar{f} \pm 1\sigma$	3σ range
$\theta_{12}/^\circ$	$33.44^{+0.77}_{-0.74}$	$31.27 - 35.86$
$\theta_{23}/^\circ$	$49.2^{+1.0}_{-1.3}$	$39.5 - 52$
$\theta_{13}/^\circ$	$8.57^{+0.13}_{-0.12}$	$8.20 - 8.97$
$\delta_{CP}/^\circ$	194^{+52}_{-25}	$105 - 405$
$\frac{\Delta m_{21}^2}{10^{-5} eV^2}$	$7.42^{+0.21}_{-0.20}$	$6.82 - 8.04$
$\frac{ \Delta m_{31}^2 }{10^{-3} eV^2}$	$2.515^{+0.028}_{-0.027}$	$2.431 - 2.599$

TABLE I. 3ν oscillation parameters obtained from different global analysis of neutrino data in normal ordering.

II. PARAMETRIZATION OF PMNS MATRIX AND NUMERICAL VALUES OF THE REQUIRED PARAMETERS

For two flavor oscillation, the mixing matrix is a 2×2 unitary matrix as shown in the following,

$$\begin{bmatrix} \nu_e \\ \nu_\mu \end{bmatrix} = \begin{bmatrix} \cos \theta & \sin \theta \\ -\sin \theta & \cos \theta \end{bmatrix} \begin{bmatrix} \nu_1 \\ \nu_2 \end{bmatrix}, \quad (3)$$

where, θ is the mixing angle.

In 3×3 case, the form of PMNS matrix U is expressed in the following manner,

$$U = \begin{bmatrix} U_{e1} & U_{e2} & U_{e3} \\ U_{\mu 1} & U_{\mu 2} & U_{\mu 3} \\ U_{\tau 1} & U_{\tau 2} & U_{\tau 3} \end{bmatrix}. \quad (4)$$

The Particle Data Group has adopted a parametrization for U known as Standard Parametrization, where U is parametrized by three mixing angles (θ_{12} , θ_{13} , θ_{23}), and one CP-violating phase(δ). Two extra CP-violating phases known as Majorana phases(α , β) are included in U , if the Majorana nature of the neutrino is considered. The standard form of U is expressed in the following manner,

$$U = \begin{bmatrix} c_{12} c_{13} & & c_{13} s_{12} \\ -c_{23} s_{12} - c_{12} s_{13} s_{23} e^{i\delta} & c_{12} c_{23} - s_{12} s_{13} s_{23} e^{i\delta} & \\ s_{12} s_{23} - c_{12} c_{23} s_{13} e^{i\delta} & -c_{12} s_{23} - s_{12} s_{13} c_{23} e^{i\delta} & \\ s_{13} e^{-i\delta} & \begin{bmatrix} e^{i\alpha} & 0 & 0 \\ 0 & e^{i\beta} & 0 \\ 0 & 0 & 1 \end{bmatrix}, & \end{bmatrix} \quad (5)$$

where, $c_{ij} = \cos \theta_{ij}$ and $s_{ij} = \sin \theta_{ij}$. The numerical values of the oscillation parameters obtained from oscillation [16] experiments are presented in Table I. However, the Majorana phases are unobservable in the oscillation experiments.

In our work, we shall deal with the normal ordering of the neutrino masses ($m_3 > m_2 > m_1$). The value of m_3 is fixed at $0.06 \text{ eV}/c^2$ and m_1 and m_2 are estimated as $0.0318 \text{ eV}/c^2$ and $0.0329 \text{ eV}/c^2$, such that $(m_1 + m_2 +$

$m_3 = 0.124 \text{ eV}/c^2$). We highlight that the sum of three neutrino masses considered in our work is consistent with the cosmological data [17–20]. For two flavor oscillation, we assume $\theta = 45^\circ$. For 3×3 case, we choose the best fit values of the parameters (see Table I) for numerical analysis and plots.

III. NEUTRINO OSCILLATION PROBABILITY INSIDE AN INFINITE SQUARE WELL POTENTIAL

we know that the nature of the particle confined in a box is steered by a parameter $L_c = \frac{\lambda_c}{2\pi}$ [21] where, λ_c is the Compton wavelength of the particle inside the well. If the well size $L >> L_c$, the behavior of the particle is considered to be non-relativistic. Now, if $L \sim L_c$ or smaller, then the nature of the particle is considered to be relativistic inside the box. In the present work, we study the neutrino oscillation probability by considering both non-relativistic and relativistic cases.

A. Non-Relativistic Case

In non-relativistic quantum mechanics, the problem of particle inside a infinite square well potential,

$$V(x) = \begin{cases} 0 & 0 < x < L \\ \infty & \text{otherwise} \end{cases}, \quad (6)$$

is a fundamental one and is governed by the Schrödinger equation [22–24]. The quantised energy of the particle in n^{th} state inside the potential is given by,

$$E_n = \frac{n^2 \pi^2 \hbar^2}{2 m L^2}, \quad (7)$$

where, m is the mass of the particle and L denotes the size of the well.

Under our consideration, an electron type neutrino is trapped inside a hypothetical infinite square well potential. We first consider two flavor oscillation so that the expression for $P_{\nu_e \rightarrow \nu_\mu}$ can be obtained as shown in the following,

$$P_{\nu_e \rightarrow \nu_\mu} = \sin^2(2\theta) \sin^2 \left[\frac{\pi^2 \hbar t}{4 L^2} \left(\frac{n_1^2}{m_1} - \frac{n_2^2}{m_2} \right) \right]. \quad (8)$$

The oscillation frequency f_{NR} can be calculated from the following expression,

$$f_{NR} = \frac{\pi \hbar}{8 L^2} \left(\frac{n_1^2}{m_1} - \frac{n_2^2}{m_2} \right) \quad (9)$$

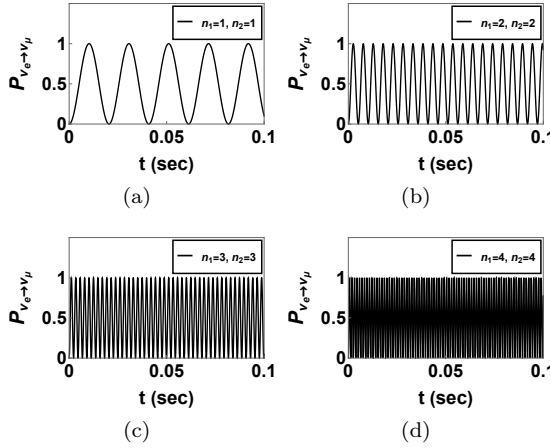


FIG. 1. (a) Shows the plot of $P_{\nu_e \rightarrow \nu_\mu}$ against t for $n_1 = 1$ and $n_2 = 1$ in case of two flavor oscillation in non-relativistic case. (b) Plot of $P_{\nu_e \rightarrow \nu_\mu}$ against t is shown when $n_1 = 2$ and $n_2 = 2$. (c) Presents the plot of $P_{\nu_e \rightarrow \nu_\mu}$ against t for $n_1 = 3$ and $n_2 = 3$. (d) Manifests the plot of $P_{\nu_e \rightarrow \nu_\mu}$ against t where $n_1 = 4$ and $n_2 = 4$. From the plots, we notice that the oscillation frequency increases as the energy of the mass eigenstates increases.

We encounter two possible cases while plotting $P_{\nu_e \rightarrow \nu_\mu}$ against t . In first case, we see that the oscillation frequency changes if the energy of the mass eigenstates increases but posses same quantum number, i.e., $n_1 = n_2$ (see Figs. 1-2). For this case, the bound set on t is $[0 - 0.1 \text{ sec}]$. In second case, we notice a change in oscillation frequency if the mass eigenstates posses different quantum number (see Figs. 3-4). The range given for t is $[0 - 0.001 \text{ sec}]$. In the present work, the quantum numbers n_1 , n_2 and n_3 are associated with mass eigenstates ν_1 , ν_2 and ν_3 respectively. The well length is set at 1 meter. A similar kind of work is done in the wave packet approach by considering the non-relativistic nature of neutrino [25].

B. Relativistic case

As we mentioned earlier, dealing with the problems related to trapping potential is challenging for relativistic scenarios. Because one may encounter a conjecture termed as Klein-Paradox. However, we may avoid Klein Paradox by considering a Lorentz scalar potential. The form of the potential considered in our work is a position-dependent mass and is given by,

$$m(x) = \begin{cases} m & 0 < x < L \\ \infty & \text{otherwise} \end{cases}. \quad (10)$$

If the spin of the neutrino is not considered, the form of the quantised energy of a particle trapped inside the potential is given by,

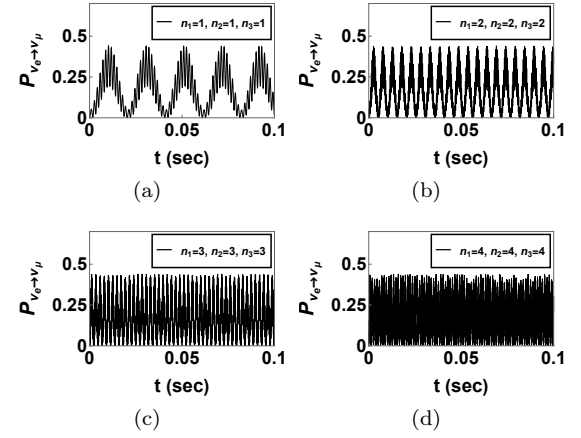


FIG. 2. (a) Displays the plot of $P_{\nu_e \rightarrow \nu_\mu}$ against t when $n_1 = 1$, $n_2 = 1$ and $n_3 = 1$ for three flavor oscillation in non-relativistic scenario. (b) Plot of $P_{\nu_e \rightarrow \nu_\mu}$ against t is shown where $n_1 = 2$, $n_2 = 2$ and $n_3 = 2$. (c) Gives the plot of $P_{\nu_e \rightarrow \nu_\mu}$ against t for $n_1 = 3$, $n_2 = 3$ and $n_3 = 3$. (d) The plot of $P_{\nu_e \rightarrow \nu_\mu}$ against t is manifested $n_1 = 4$, $n_2 = 4$ and $n_3 = 4$. From the plots, we see a increase in oscillation frequency with the increase in energy of the mass eigenstates.

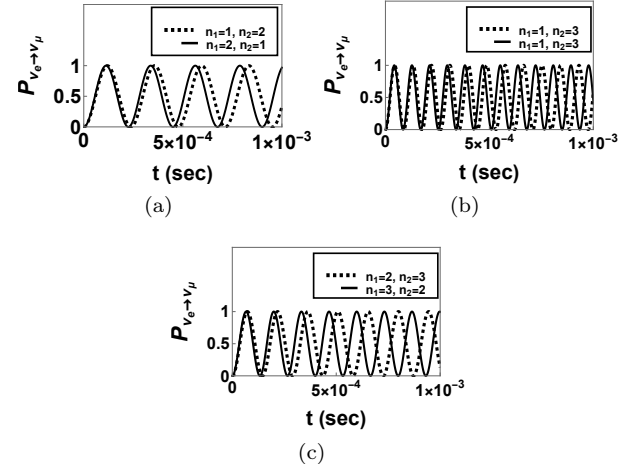


FIG. 3. (a) Presents the plot of $P_{\nu_e \rightarrow \nu_\mu}$ against t for $n_1 = 1$ and $n_2 = 2$ and vice-versa for two flavor oscillation in non-relativistic case. (b) Plot of $P_{\nu_e \rightarrow \nu_\mu}$ against t is shown for $n_1 = 1$ and $n_2 = 3$ and vice-versa. (c) Manifests the plot of $P_{\nu_e \rightarrow \nu_\mu}$ against t for $n_1 = 2$ and $n_2 = 3$ and vice-versa. From the plots, we find that the oscillation frequency changes with the change in energy of the mass eigenstates.

$$E_n = \sqrt{\hbar^2 c^2 k_n^2 + m^2 c^4}, \quad k_n = \frac{n\pi}{L}, \quad (11)$$

where, $n = 1, 2, 3, \dots$ etc. Now, if we consider a relativistic electron type neutrino is trapped in a infinite square-well potential, the expression for $P_{\nu_e \rightarrow \nu_\mu}$ (in case of two flavor oscillation) can be obtained as shown in the following,

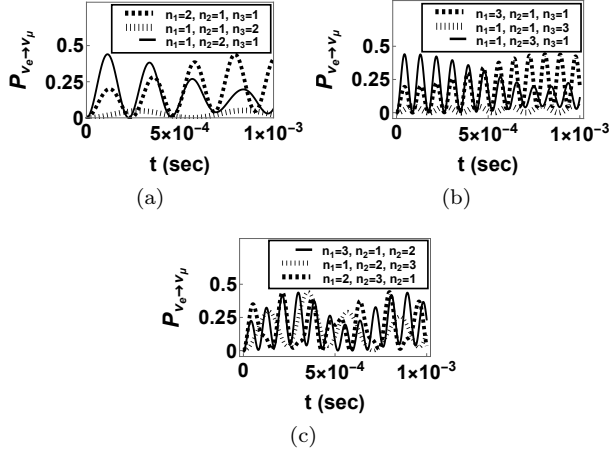


FIG. 4. (a) Shows the plot of $P_{\nu_e \rightarrow \nu_\mu}$ against t for three flavor oscillation in non-relativistic case, where, n_1 , n_2 and n_3 can have values $(1, 1, 2)$, $(1, 2, 1)$ and $(2, 1, 1)$ respectively. (b) Gives the plot of $P_{\nu_e \rightarrow \nu_\mu}$ against t for the combinations of quantum numbers $(1, 1, 3)$, $(1, 3, 1)$ and $(3, 1, 1)$ respectively. (c) Plot of $P_{\nu_e \rightarrow \nu_\mu}$ against t is shown where n_1 , n_2 and n_3 are chosen to be $(1, 2, 3)$, $(2, 3, 1)$ and $(3, 1, 2)$ respectively. From the plots, it is clear that the frequency as well the amplitude of the oscillation changes as the energy of the mass eigenstates changes.

Mass Eigenstates	$k_1(m^{-1})$	$k_2(m^{-1})$	$k_3(m^{-1})$
m_1	220185	502241	805122
m_2	221522	503187	805770
m_3	246048	523767	820822

TABLE II. Numerical values of k_1 , k_2 and k_3 with respect to m_1 , m_2 and m_3 respectively.

$$P_{\nu_e \rightarrow \nu_\mu} = \sin^2(2\theta) \sin^2 \left[\frac{t}{2\hbar} \left\{ \left(\frac{n_1^2 \pi^2 \hbar^2 c^2}{L^2} + m_1^2 c^4 \right)^{\frac{1}{2}} - \left(\frac{n_2^2 \pi^2 \hbar^2 c^2}{L^2} + m_2^2 c^4 \right)^{\frac{1}{2}} \right\} \right] \quad (12)$$

The oscillation frequency for Klein-Gordon case f_{KG} is given by,

$$f_{KG} = \frac{1}{4\pi\hbar} \left[\left(\frac{n_1^2 \pi^2 \hbar^2 c^2}{L^2} + m_1^2 c^4 \right)^{\frac{1}{2}} - \left(\frac{n_2^2 \pi^2 \hbar^2 c^2}{L^2} + m_2^2 c^4 \right)^{\frac{1}{2}} \right] \quad (13)$$

When we consider the spin half nature of the neutrinos, the neutrino oscillation can be studied by considering the Dirac equation. But then things become a little complicated as we encounter a transcendental equation for the allowed wave number of quantized energy states. The energy of a Dirac particle trapped inside a potential well of length L is expressed in the following manner,

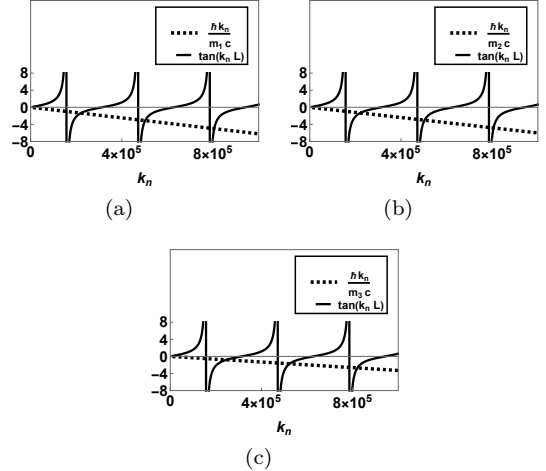


FIG. 5. (a) Presents the plot of $\tan(kL)$ and $\frac{\hbar k_n}{m_1 c}$ against the wave number k . (b) The plot of $\tan(kL)$ and $\frac{\hbar k_n}{m_2 c}$ against the wave number k is displayed. (c) Manifests the plot of $\tan(kL)$ and $\frac{\hbar k_n}{m_3 c}$ against the wave number k . From figure, we encounter three intersection points of the above said expressions. From these points, the values of k_1 , k_2 and k_3 are calculated for three mass eigenstates.

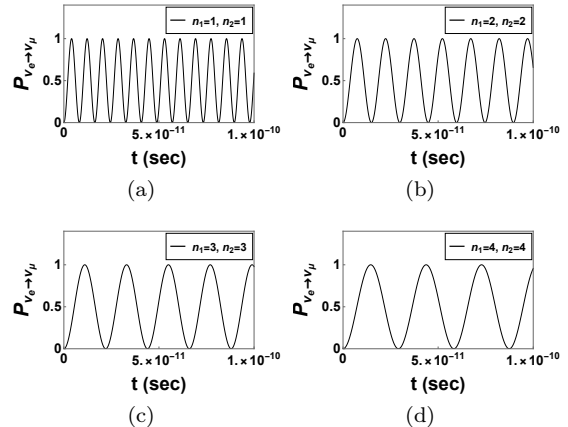


FIG. 6. (a) Shows the plot of $P_{\nu_e \rightarrow \nu_\mu}$ against t where, $n_1 = 1$ and $n_2 = 1$ for two flavor oscillation in relativistic case (Klein-Gordon). (b) The plot of $P_{\nu_e \rightarrow \nu_\mu}$ against t is manifested for $n_1 = 2$ and $n_2 = 2$. (c) Displays the plot of $P_{\nu_e \rightarrow \nu_\mu}$ against t when $n_1 = 3$ and $n_2 = 3$. (d) The plot of $P_{\nu_e \rightarrow \nu_\mu}$ against t is presented, where, $n_1 = 4$ and $n_2 = 4$ respectively. From the plots, we notice a decrease in the oscillation frequency increases as the energy of the mass eigenstates increases.

$$E_n = \sqrt{\hbar^2 c^2 k_n^2 + m^2 c^4}, \quad k_n \neq 0 \quad (14)$$

where, k_n denotes the n^{th} solution of the transcendental equation as shown below,

$$\tan(k_n L) = - \frac{\hbar k_n}{mc} \quad (15)$$

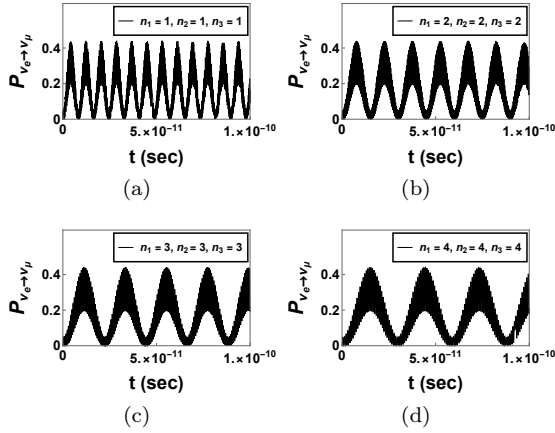


FIG. 7. (a) Shows the plot of $P_{\nu_e \rightarrow \nu_\mu}$ against t , where, $n_1 = 1$, $n_2 = 1$ and $n_3 = 1$ for three flavor oscillation in relativistic scenario (Klein-Gordon). (b) The plot of $P_{\nu_e \rightarrow \nu_\mu}$ against t is manifested for $n_1 = 2$, $n_2 = 2$ and $n_3 = 2$. (c) Presents the plot of $P_{\nu_e \rightarrow \nu_\mu}$ against t for $n_1 = 3$, $n_2 = 3$ and $n_3 = 3$ respectively. (d) Displays the plot of $P_{\nu_e \rightarrow \nu_\mu}$ against t , where, $n_1 = 4$, $n_2 = 4$ and $n_3 = 4$. From the plots, we observe that the oscillation frequency decreases with the increase in energy of the mass eigenstates.

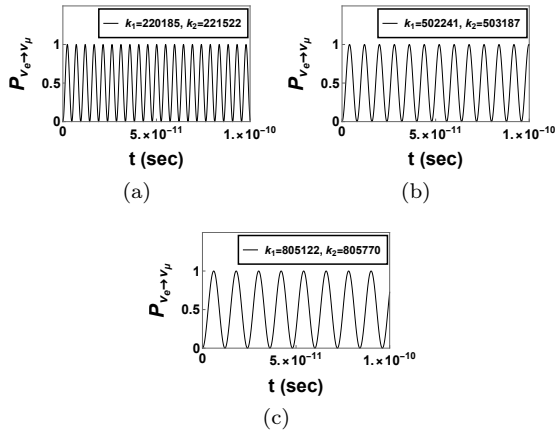


FIG. 8. (a) Displays the plot of $P_{\nu_e \rightarrow \nu_\mu}$ against t where, $k_1 = 220185 m^{-1}$ and $k_2 = 221522 m^{-1}$ for two flavor oscillation in relativistic case (Dirac). (b) Presents the plot of $P_{\nu_e \rightarrow \nu_\mu}$ against t for $k_1 = 502241 m^{-1}$ and $k_2 = 503187 m^{-1}$. (c) Manifests the plot of $P_{\nu_e \rightarrow \nu_\mu}$ against t when $k_1 = 805122 m^{-1}$ and $k_2 = 805770 m^{-1}$. From the plots, we find that oscillation frequency decreases with the increase in the energy of the mass eigenstates.

However, we may solve Eq.(15) graphically (see Fig. 5) and obtain the numerical values for k_n (see Table II). In the present work, k_1 , k_2 and k_3 are the wave number associated with the corresponding mass eigenstates ν_1 , ν_2 and ν_3 respectively. Now, if we consider two flavor neutrino oscillation, the expression for $P_{\nu_e \rightarrow \nu_\mu}$ can be obtained as shown in the following,

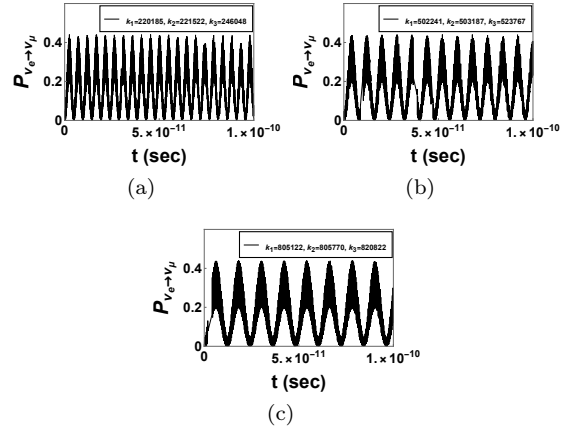


FIG. 9. (a) The plot of $P_{\nu_e \rightarrow \nu_\mu}$ against t is shown, where, $k_1 = 220185 m^{-1}$, $k_2 = 221522 m^{-1}$ and $k_3 = 246048 m^{-1}$ for three flavor oscillation in relativistic scenario (Dirac). (b) Presents the plot of $P_{\nu_e \rightarrow \nu_\mu}$ against t for $k_1 = 502241 m^{-1}$, $k_2 = 503187 m^{-1}$ and $k_3 = 523767 m^{-1}$. (c) Manifests the plot of $P_{\nu_e \rightarrow \nu_\mu}$ against t when $k_1 = 805122 m^{-1}$, $k_2 = 805770 m^{-1}$ and $k_3 = 820822 m^{-1}$ respectively. From the plots, we perceive that the oscillation frequency decreases when the energy of the mass eigenstates increases.

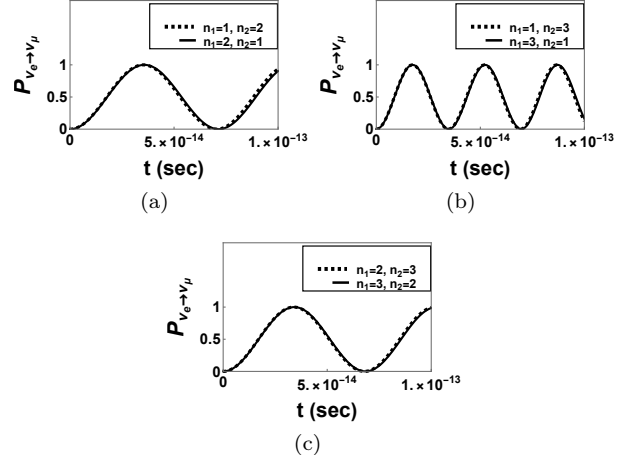


FIG. 10. (a) Gives the plot of $P_{\nu_e \rightarrow \nu_\mu}$ against t for $n_1 = 1$ and $n_2 = 2$ and vice-versa when two flavor oscillation is considered in relativistic case (Klein-Gordon). (b) Presents the plot of $P_{\nu_e \rightarrow \nu_\mu}$ against t for $n_1 = 1$ and $n_2 = 3$ and vice-versa. (c) Displays the plot of $P_{\nu_e \rightarrow \nu_\mu}$ against t , where, $n_1 = 2$ and $n_2 = 3$ and vice-versa. From the figure, we notice rarely any change in oscillation frequency for above mentioned energies.

$$P_{\nu_e \rightarrow \nu_\mu} = \sin^2(2\theta) \sin^2 \left[\frac{t}{2\hbar} \left\{ \left(\hbar^2 c^2 k_1^2 + m_1^2 c^4 \right)^{\frac{1}{2}} - \left(\hbar^2 c^2 k_2^2 + m_2^2 c^4 \right)^{\frac{1}{2}} \right\} \right], \quad (16)$$

where, the oscillation frequency f_D can be calculated from the expression as shown in the following,

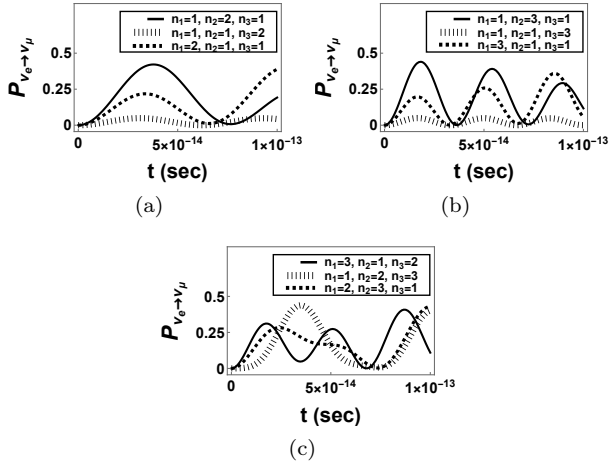


FIG. 11. (a) Presents the plot of $P_{\nu_e \rightarrow \nu_\mu}$ against t when three flavor oscillation in relativistic case is considered (Klein-Gordon), where, n_1 , n_2 and n_3 can have values $(1, 1, 2)$, $(1, 2, 1)$ and $(2, 1, 1)$ respectively. (b) Shows the plot of $P_{\nu_e \rightarrow \nu_\mu}$ against t for the combinations of quantum numbers $(1, 1, 3)$, $(1, 3, 1)$ and $(3, 1, 1)$ respectively. (c) Plot of $P_{\nu_e \rightarrow \nu_\mu}$ against t is manifested where the values of n_1 , n_2 and n_3 are chosen to be $(1, 2, 3)$, $(2, 3, 1)$ and $(3, 1, 2)$ respectively. From the plots, we observe that the frequency and the amplitude of oscillation changes with the change in energy of the mass eigenstates.

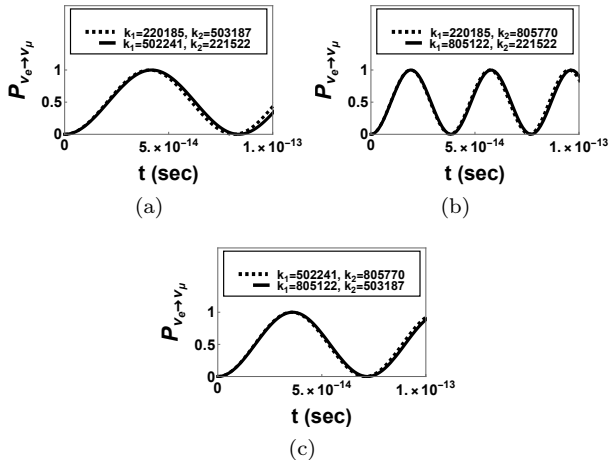


FIG. 12. (a) Manifests the plot of $P_{\nu_e \rightarrow \nu_\mu}$ against t for the combinations $k_1 = 220185 \text{ m}^{-1}$, $k_2 = 503187 \text{ m}^{-1}$ and $k_1 = 502241 \text{ m}^{-1}$, $k_2 = 221522 \text{ m}^{-1}$ when two flavor oscillation is considered in relativistic case (Dirac). (b) Displays the plot of $P_{\nu_e \rightarrow \nu_\mu}$ against t for the combinations of the values of the wave number; $k_1 = 220185 \text{ m}^{-1}$, $k_2 = 805770 \text{ m}^{-1}$ and $k_1 = 805122 \text{ m}^{-1}$, $k_2 = 221522 \text{ m}^{-1}$. (c) Presents the plot of $P_{\nu_e \rightarrow \nu_\mu}$ against t , where, the wave number k can have values $k_1 = 502241 \text{ m}^{-1}$, $k_2 = 805770 \text{ m}^{-1}$ and $k_1 = 805122 \text{ m}^{-1}$, $k_2 = 503187 \text{ m}^{-1}$. From the figure, we observe very small change in oscillation frequency for above mentioned energies.

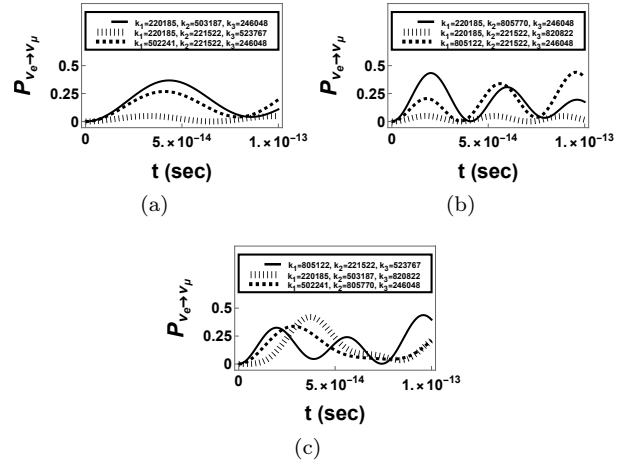


FIG. 13. (a) The plot of $P_{\nu_e \rightarrow \nu_\mu}$ against t is shown for three flavor oscillation in relativistic case (Dirac) for combinations of the wave number ($k_1 = 220185 \text{ m}^{-1}$, $k_2 = 503187 \text{ m}^{-1}$, $k_3 = 246048 \text{ m}^{-1}$), ($k_1 = 220185 \text{ m}^{-1}$, $n_2 = 221522 \text{ m}^{-1}$, $k_3 = 523767 \text{ m}^{-1}$) and ($k_1 = 502241 \text{ m}^{-1}$, $k_2 = 221522 \text{ m}^{-1}$, $k_3 = 246048 \text{ m}^{-1}$). (b) Gives the plot of $P_{\nu_e \rightarrow \nu_\mu}$ against t where the combinations of quantum numbers are ($k_1 = 220185 \text{ m}^{-1}$, $n_2 = 805770 \text{ m}^{-1}$, $k_3 = 246048 \text{ m}^{-1}$), ($k_1 = 220185 \text{ m}^{-1}$, $k_2 = 221522 \text{ m}^{-1}$, $k_3 = 820822 \text{ m}^{-1}$) and ($k_1 = 805122 \text{ m}^{-1}$, $k_2 = 221522 \text{ m}^{-1}$, $k_3 = 246048 \text{ m}^{-1}$). (c) Displays the plot of $P_{\nu_e \rightarrow \nu_\mu}$ against t , where, the values of k_1 , k_2 and k_3 are chosen in the following combinations, ($k_1 = 805122 \text{ m}^{-1}$, $n_2 = 221522 \text{ m}^{-1}$, $k_3 = 523767 \text{ m}^{-1}$), ($k_1 = 220185 \text{ m}^{-1}$, $k_2 = 503187 \text{ m}^{-1}$, $k_3 = 820822 \text{ m}^{-1}$) and ($k_1 = 502241 \text{ m}^{-1}$, $k_2 = 805770 \text{ m}^{-1}$, $k_3 = 246048 \text{ m}^{-1}$). From the plots, we observe that the frequency and the amplitude of oscillation changes when the energy of the mass eigenstates changes.

$$f_D = \frac{1}{4\pi\hbar} \left[\left(\hbar^2 c^2 k_1^2 + m_1^2 c^4 \right)^{\frac{1}{2}} - \left(\hbar^2 c^2 k_2^2 + m_2^2 c^4 \right)^{\frac{1}{2}} \right] \quad (17)$$

Similar to the non-relativistic case, we encounter two possible scenarios while plotting $P_{\nu_e \rightarrow \nu_\mu}$ against t . In first case, we observe that the frequency of oscillation decreases as the energy of the mass eigenstates increases where the mass eigenstates posses same quantum number(see Figs. 6-9). For this case, the range given for t is $[0 - 10^{-10} \text{ sec}]$. In the second case, we find that the oscillation frequency changes if the neutrino mass eigenstates posses different quantum numbers(see Figs. 10-13). The bound set on t for this case is $[0 - 10^{-13} \text{ sec}]$. For relativistic case, the well length is set at 10^{-4} meter.

Further, if we look at the fact that neutrinos are electromagnetically neutral particles, they might resemble their own anti-particle state i.e., a Majorana Particle [26, 27]. However, the scenarios remain akin to the Dirac

case as we perceive the same transcendental equation for the allowed wave number k_n [28]. Apart from that, we obtain plots of $P_{\nu_e \rightarrow \nu_\mu}$ against t analogous to Dirac case.

IV. COMPARISON OF OSCILLATION FREQUENCY FOR RELATIVISTIC AND NON-RELATIVISTIC CASE

If the energy of the mass eigenstates increases but possess the same quantum number ($n_1 = n_2$), we notice a significant difference in oscillation frequency for the relativistic and non-relativistic case. In the former case, we observe that the frequency of oscillation decreases with an increase in the energy of the mass eigenstates. But in the latter case, the frequency increases as the energy of the mass eigenstates increases. In addition to this, the oscillation frequency almost remains the same as the mass eigenstates possess different quantum numbers for two flavor oscillations in a relativistic case.

V. CONDITION FOR NO FLAVOR OSCILLATION

In the theory of standard neutrino oscillation, where the neutrino travels in free space, the oscillation stops when $\Delta m_{21}^2 = 0$. This signifies that the neutrino mass eigenvalues cannot be degenerate. But in our approach, i.e., when the neutrino is confined inside a potential, we encounter non-zero oscillation probability even if $\Delta m_{21}^2 = 0$. This is because the quantum numbers associated with the mass eigenstates may be different. However, the oscillation may stop for some specific conditions.

In non-relativistic scenario, we exploit Eq. (8) and Eq. (28)(see appendix) to draw a important consequence. If two neutrino mass eigenstates posses different quantum number ($n_1 \neq n_2$), we witness non zero value of $P_{\nu_e \rightarrow \nu_\mu}$ even if the neutrino mass eigenstates are degenerate i.e., $m_1 = m_2$ (see Figs. 14-15).

From Eq. (8), we see that in two flavor oscillation, the oscillation will not occur for the following condition,

$$m_1 = \left(\frac{n_1^2}{n_2^2} \right) m_2. \quad (18)$$

In 3×3 case, the condition for zero oscillation probability is shown below,

$$m_3 = \left(\frac{n_3^2}{n_1^2} \right) m_1 = \left(\frac{n_3^2}{n_2^2} \right) m_2. \quad (19)$$

In relativistic scenario, we obtain result similar to the non-relativistic case. From Eq. (12-16) and (29-30)(see appendix), we see non-zero oscillation probability $P_{\nu_e \rightarrow \nu_\mu}$

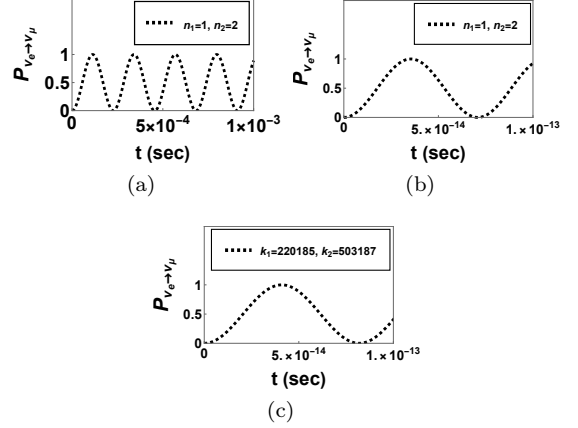


FIG. 14. (a) Presents the plot of $P_{\nu_e \rightarrow \nu_\mu}$ against t for $m_1 = m_2$ in case of two flavor oscillation in non-relativistic case. (b) Displays the plot of $P_{\nu_e \rightarrow \nu_\mu}$ against t for two flavor oscillation in relativistic case (Klein-Gordon), where, $m_1 = m_2$. (c) Shows the plot of $P_{\nu_e \rightarrow \nu_\mu}$ against t for $m_1 = m_2$ for two flavor oscillation in relativistic case (Dirac). From the plots, we notice a non-zero oscillation probability even if the mass eigenvalues are degenerate.

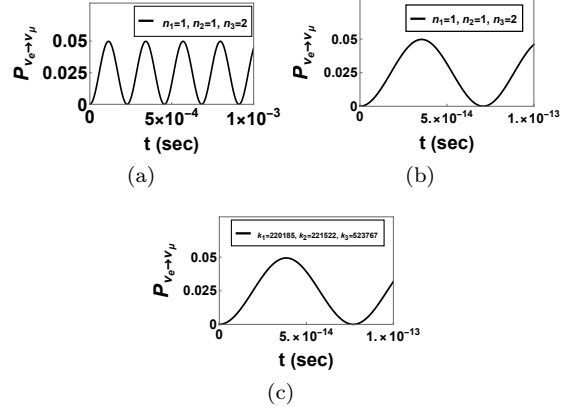


FIG. 15. (a) The plot of $P_{\nu_e \rightarrow \nu_\mu}$ against t is manifested for $m_1 = m_2 = m_3$, when three flavor oscillation in non-relativistic case is considered. (b) Presents the plot of $P_{\nu_e \rightarrow \nu_\mu}$ against t where, $m_1 = m_2 = m_3$ for three flavor oscillation in relativistic case (Klein-Gordon). (c) Displays the plot of $P_{\nu_e \rightarrow \nu_\mu}$ against t for three flavor oscillation in relativistic case (Dirac) for $m_1 = m_2 = m_3$. From the plots, we see that the non-zero oscillation probability exists for degenerate neutrino mass eigenvalues.

for degenerate neutrino mass eigenstates (see Figs. 14-15). However, the oscillation will stop for some conditions as discussed below.

In two flavor oscillation, if we consider Klein-Gordon case, we find that the oscillation will stop for the condition as shown in the following,

$$\Delta m_{21}^2 = \frac{\pi^2 \hbar^2}{L^2 c^2} (n_1^2 - n_2^2). \quad (20)$$

Also, in the Dirac case, we exploit Eq. (16) and perceive the condition for zero probability of conversion as shown below,

$$\Delta m_{21}^2 = \frac{\hbar^2}{c^2} (k_1^2 - k_2^2). \quad (21)$$

In 3×3 scenario, the conditions for zero oscillation probability by considering Klein-Gordon case are shown in the following,

$$\Delta m_{21}^2 = (n_1^2 - n_2^2) \left(\frac{\pi^2 \hbar^2}{L^2 c^2} \right) \quad (22)$$

$$\Delta m_{31}^2 = (n_1^2 - n_3^2) \left(\frac{\pi^2 \hbar^2}{L^2 c^2} \right) \quad (23)$$

$$\Delta m_{32}^2 = (n_2^2 - n_3^2) \left(\frac{\pi^2 \hbar^2}{L^2 c^2} \right) \quad (24)$$

If we consider the Dirac case, then the conditions for which the oscillation will not occur are given below,

$$\Delta m_{21}^2 = (k_1^2 - k_2^2) \left(\frac{\hbar^2}{c^2} \right) \quad (25)$$

$$\Delta m_{31}^2 = (k_1^2 - k_3^2) \left(\frac{\hbar^2}{c^2} \right) \quad (26)$$

$$\Delta m_{32}^2 = (k_2^2 - k_3^2) \left(\frac{\hbar^2}{c^2} \right) \quad (27)$$

We see that when the neutrino is trapped inside a infinite square well potential, the quantum numbers associated with the mass eigenstates play a crucial role in the flavor oscillation phenomenon.

VI. SUMMARY AND DISCUSSION

In our work, we follow Pontecorvo's approach and set a thought experiment to study neutrino oscillation inside a confined region. We formulate our work by considering both relativistic and non-relativistic frameworks. The oscillation is expressed with respect to time and a few important consequences are generated. In both the frameworks, we find that there exists a non-zero oscillation probability for degenerate neutrino mass eigenstates. Apart from this, $P_{\nu_e \rightarrow \nu_\mu}$ is plotted against time for two possible cases; the mass eigenstates possess the same and different quantum numbers. For the first case, we encounter a significant difference between the oscillation frequency for relativistic and non-relativistic scenarios. For the relativistic scenario, we find that the oscillation frequency decreases as the energy of the mass eigenstates increases, while for the non-relativistic scenario, we see an increase in oscillation frequency as the energy of the mass eigenstates increases. In the context of two flavor oscillations concerning the second case, we observe a change in oscillation frequency when the energies of the mass eigenstates change. However, for the three-flavor oscillation, we observe a change in both frequency and amplitude of oscillation as the energy of the mass eigenstates changes. Towards the end of our work, we highlight some conditions for which the neutrino oscillation stops for both the relativistic and non-relativistic cases.

VII. ACKNOWLEDGEMENT

The research work of Pralay Chakraborty is supported by Innovation in Science Pursuit for Inspired Research (INSPIRE), Department of Science and Technology, Government of India, New Delhi vide grant No. IF190651.

[1] S. L. Glashow, Partial Symmetries of Weak Interactions, *Nucl. Phys.* **22**, 579 (1961).

[2] S. Weinberg, A Model of Leptons, *Phys. Rev. Lett.* **19**, 1264 (1967).

[3] M. Herrero, The Standard model, *NATO Sci. Ser. C* **534**, 1 (1999), arXiv:hep-ph/9812242.

[4] H. Fritzsch, Neutrino Masses and Flavor Mixing, *Mod. Phys. Lett. A* **30**, 1530012 (2015), arXiv:1503.01857 [hep-ph].

[5] S. Morisi and J. W. F. Valle, Neutrino masses and mixing: a flavour symmetry roadmap, *Fortsch. Phys.* **61**, 466 (2013), arXiv:1206.6678 [hep-ph].

[6] Y. Farzan and M. Tortola, Neutrino oscillations and Non-Standard Interactions, *Front. in Phys.* **6**, 10 (2018), arXiv:1710.09360 [hep-ph].

[7] S. A. R. Ellis, K. J. Kelly, and S. W. Li, Current and Future Neutrino Oscillation Constraints on Leptonic Unitarity, *JHEP* **12**, 068, arXiv:2008.01088 [hep-ph].

[8] G. Fantini, A. Gallo Rosso, F. Vissani, and V. Zema, Introduction to the Formalism of Neutrino Oscillations, *Adv. Ser. Direct. High Energy Phys.* **28**, 37 (2018), arXiv:1802.05781 [hep-ph].

[9] A. Calogeracos and N. Dombey, Klein tunneling and the Klein paradox, *Int. J. Mod. Phys. A* **14**, 631 (1999), arXiv:quant-ph/9806052.

[10] N. Dombey and A. Calogeracos, Seventy years of the Klein paradox, *Phys. Rept.* **315**, 41 (1999).

- [11] A. Hansen and F. Ravndal, Klein's Paradox and Its Resolution, *Phys. Scripta* **23**, 1036 (1981).
- [12] R. K. Su, G. G. Siu, and X. Chou, Barrier penetration and Klein Paradox, *J. Phys. A* **26**, 1001 (1993).
- [13] A. Calogeracos and N. Dombey, History and physics of the Klein paradox, *Contemp. Phys.* **40**, 313 (1999), arXiv:quant-ph/9905076.
- [14] P. Alberto, S. Das, and E. C. Vagenas, Relativistic particle in a three-dimensional box, *Phys. Lett. A* **375**, 1436 (2011), arXiv:1102.3192 [quant-ph].
- [15] P. Alberto, S. Das, and E. C. Vagenas, Relativistic particle in a box: Klein-Gordon versus Dirac equations, *Eur. J. Phys.* **39**, 025401 (2018), arXiv:1711.06313 [quant-ph].
- [16] I. Esteban, M. C. Gonzalez-Garcia, M. Maltoni, T. Schwetz, and A. Zhou, The fate of hints: updated global analysis of three-flavor neutrino oscillations, *JHEP* **09**, 178, arXiv:2007.14792 [hep-ph].
- [17] A. Loureiro *et al.*, On The Upper Bound of Neutrino Masses from Combined Cosmological Observations and Particle Physics Experiments, *Phys. Rev. Lett.* **123**, 081301 (2019), arXiv:1811.02578 [astro-ph.CO].
- [18] A. Upadhye, Neutrino mass and dark energy constraints from redshift-space distortions, *JCAP* **05**, 041, arXiv:1707.09354 [astro-ph.CO].
- [19] S. Roy Choudhury and S. Hannestad, Updated results on neutrino mass and mass hierarchy from cosmology with Planck 2018 likelihoods, *JCAP* **07**, 037, arXiv:1907.12598 [astro-ph.CO].
- [20] C. Yèche, N. Palanque-Delabrouille, J. Baur, and H. du Mas des Bourboux, Constraints on neutrino masses from Lyman-alpha forest power spectrum with BOSS and XQ-100, *JCAP* **06**, 047, arXiv:1702.03314 [astro-ph.CO].
- [21] P. Alberto, C. Fiolhais, and V. M. S. Gil, Relativistic particle in a box, *European Journal of Physics* **17**, 19 (1996).
- [22] H. J. W. Müller-Kirsten, *Introduction to Quantum Mechanics: Schrödinger Equation and Path Integral* (World Scientific, 2012).
- [23] L. D. Landau and E. M. Lifshits, *Quantum Mechanics: Non-Relativistic Theory*, Course of Theoretical Physics, Vol. v.3 (Butterworth-Heinemann, Oxford, 1991).
- [24] J. J. Sakurai and J. Napolitano, *Modern Quantum Mechanics*, Quantum physics, quantum information and quantum computation (Cambridge University Press, 2020).
- [25] L. Johns, Neutrino oscillations in a trapping potential, *Int. J. Mod. Phys. A* **34**, 1950160 (2019), arXiv:1906.01673 [hep-ph].
- [26] H. Arodź, Relativistic Quantum Mechanics of the Majorana Particle, *Acta Phys. Polon. B* **50**, 2165 (2019), arXiv:2002.07482 [quant-ph].
- [27] L. Borsten and M. J. Duff, Majorana Fermions in Particle Physics, Solid State and Quantum Information, *Subnucl. Ser.* **53**, 77 (2017), arXiv:1612.01371 [hep-th].
- [28] S. De Vincenzo, On real solutions of the Dirac equation for a one-dimensional Majorana particle, *Results Phys.* **15**, 102598 (2019), arXiv:2007.03072 [quant-ph].

VIII. APPENDIX

In non-relativistic case, the expression of $P_{\nu_e \rightarrow \nu_\mu}$ for three flavor oscillation can be obtained as shown below,

$$\begin{aligned}
P_{\nu_e \rightarrow \nu_\mu} = & -4 \operatorname{Re} (U_{e1} U_{\mu1}^* U_{e2}^* U_{\mu2}) \sin^2 \left[\frac{\pi^2 \hbar t}{4L^2} \left(\frac{n_2^2}{m_2} - \frac{n_1^2}{m_1} \right) \right] \\
& + 2 \operatorname{Im} (U_{e1} U_{\mu1}^* U_{e2}^* U_{\mu2}) \sin \left[\frac{\pi^2 \hbar t}{2L^2} \left(\frac{n_2^2}{m_2} - \frac{n_1^2}{m_1} \right) \right] \\
& - 4 \operatorname{Re} (U_{e1} U_{\mu1}^* U_{e3}^* U_{\mu3}) \sin^2 \left[\frac{\pi^2 \hbar t}{4L^2} \left(\frac{n_3^2}{m_3} - \frac{n_1^2}{m_1} \right) \right] \\
& + 2 \operatorname{Im} (U_{e1} U_{\mu1}^* U_{e3}^* U_{\mu3}) \sin \left[\frac{\pi^2 \hbar t}{2L^2} \left(\frac{n_3^2}{m_3} - \frac{n_1^2}{m_1} \right) \right] \\
& - 4 \operatorname{Re} (U_{e2} U_{\mu2}^* U_{e3}^* U_{\mu3}) \sin^2 \left[\frac{\pi^2 \hbar t}{4L^2} \left(\frac{n_3^2}{m_3} - \frac{n_2^2}{m_2} \right) \right] \\
& + 2 \operatorname{Im} (U_{e2} U_{\mu2}^* U_{e3}^* U_{\mu3}) \sin \left[\frac{\pi^2 \hbar t}{2L^2} \left(\frac{n_3^2}{m_3} - \frac{n_2^2}{m_2} \right) \right]
\end{aligned} \tag{28}$$

For relativistic case, we may derive the expression of $P_{\nu_e \rightarrow \nu_\mu}$ for three flavor oscillation considering the Klein-Gordon equation in the following way,

$$\begin{aligned}
P_{\nu_e \rightarrow \nu_\mu} = & -4 \operatorname{Re} (U_{e1} U_{\mu1}^* U_{e2}^* U_{\mu2}) \sin^2 \left[\frac{t}{2\hbar} \left\{ \left(\frac{n_2^2 \pi^2 \hbar^2 c^2}{L^2} \right. \right. \right. \\
& \left. \left. \left. + m_2^2 c^4 \right)^{\frac{1}{2}} - \left(\frac{n_1^2 \pi^2 \hbar^2 c^2}{L^2} + m_1^2 c^4 \right)^{\frac{1}{2}} \right\} \right] \\
& + 2 \operatorname{Im} (U_{e1} U_{\mu1}^* U_{e2}^* U_{\mu2}) \sin \left[\frac{t}{\hbar} \left\{ \left(\frac{n_2^2 \pi^2 \hbar^2 c^2}{L^2} \right. \right. \right. \\
& \left. \left. \left. + m_2^2 c^4 \right)^{\frac{1}{2}} - \left(\frac{n_1^2 \pi^2 \hbar^2 c^2}{L^2} + m_1^2 c^4 \right)^{\frac{1}{2}} \right\} \right] \\
& - 4 \operatorname{Re} (U_{e1} U_{\mu1}^* U_{e3}^* U_{\mu3}) \sin^2 \left[\frac{t}{2\hbar} \left\{ \left(\frac{n_3^2 \pi^2 \hbar^2 c^2}{L^2} \right. \right. \right. \\
& \left. \left. \left. + m_3^2 c^4 \right)^{\frac{1}{2}} - \left(\frac{n_1^2 \pi^2 \hbar^2 c^2}{L^2} + m_1^2 c^4 \right)^{\frac{1}{2}} \right\} \right] \\
& + 2 \operatorname{Im} (U_{e1} U_{\mu1}^* U_{e3}^* U_{\mu3}) \sin \left[\frac{t}{\hbar} \left\{ \left(\frac{n_3^2 \pi^2 \hbar^2 c^2}{L^2} \right. \right. \right. \\
& \left. \left. \left. + m_3^2 c^4 \right)^{\frac{1}{2}} - \left(\frac{n_1^2 \pi^2 \hbar^2 c^2}{L^2} + m_1^2 c^4 \right)^{\frac{1}{2}} \right\} \right] \\
& - 4 \operatorname{Re} (U_{e2} U_{\mu2}^* U_{e3}^* U_{\mu3}) \sin^2 \left[\frac{t}{2\hbar} \left\{ \left(\frac{n_3^2 \pi^2 \hbar^2 c^2}{L^2} \right. \right. \right. \\
& \left. \left. \left. + m_3^2 c^4 \right)^{\frac{1}{2}} - \left(\frac{n_2^2 \pi^2 \hbar^2 c^2}{L^2} + m_2^2 c^4 \right)^{\frac{1}{2}} \right\} \right] \\
& + 2 \operatorname{Im} (U_{e2} U_{\mu2}^* U_{e3}^* U_{\mu3}) \sin \left[\frac{t}{\hbar} \left\{ \left(\frac{n_3^2 \pi^2 \hbar^2 c^2}{L^2} \right. \right. \right. \\
& \left. \left. \left. + m_3^2 c^4 \right)^{\frac{1}{2}} - \left(\frac{n_2^2 \pi^2 \hbar^2 c^2}{L^2} + m_2^2 c^4 \right)^{\frac{1}{2}} \right\} \right]
\end{aligned} \tag{29}$$

Now, if we consider the spin of neutrino, the Dirac equa-

tion comes into play. The expression for $P_{\nu_e \rightarrow \nu_\mu}$ can be obtained for three flavor oscillation considering the Dirac equation is expressed in the following manner,

$$\begin{aligned}
P_{\nu_e \rightarrow \nu_\mu} = & -4 \operatorname{Re} (U_{e1} U_{\mu 1}^* U_{e2}^* U_{\mu 2}) \sin^2 \left[\frac{t}{2\hbar} \left\{ (k_2^2 \hbar^2 c^2 \right. \right. \\
& \left. \left. + m_2^2 c^4)^{\frac{1}{2}} - (k_1^2 \hbar^2 c^2 + m_1^2 c^4)^{\frac{1}{2}} \right\} \right] \\
& + 2 \operatorname{Im} (U_{e1} U_{\mu 1}^* U_{e2}^* U_{\mu 2}) \sin \left[\frac{t}{\hbar} \left\{ (k_2^2 \hbar^2 c^2 \right. \right. \\
& \left. \left. + m_2^2 c^4)^{\frac{1}{2}} - (k_1^2 \hbar^2 c^2 + m_1^2 c^4)^{\frac{1}{2}} \right\} \right] \\
& - 4 \operatorname{Re} (U_{e1} U_{\mu 1}^* U_{e3}^* U_{\mu 3}) \sin^2 \left[\frac{t}{2\hbar} \left\{ (k_3^2 \hbar^2 c^2 \right. \right. \\
& \left. \left. + m_3^2 c^4)^{\frac{1}{2}} - (k_1^2 \hbar^2 c^2 + m_1^2 c^4)^{\frac{1}{2}} \right\} \right] \\
& + 2 \operatorname{Im} (U_{e1} U_{\mu 1}^* U_{e2}^* U_{\mu 2}) \sin \left[\frac{t}{\hbar} \left\{ (k_2^2 \hbar^2 c^2 \right. \right. \\
& \left. \left. + m_2^2 c^4)^{\frac{1}{2}} - (k_1^2 \hbar^2 c^2 + m_1^2 c^4)^{\frac{1}{2}} \right\} \right] \\
& - 4 \operatorname{Re} (U_{e2} U_{\mu 2}^* U_{e3}^* U_{\mu 3}) \sin^2 \left[\frac{t}{2\hbar} \left\{ (k_3^2 \hbar^2 c^2 \right. \right. \\
& \left. \left. + m_3^2 c^4)^{\frac{1}{2}} - (k_2^2 \hbar^2 c^2 + m_2^2 c^4)^{\frac{1}{2}} \right\} \right] \\
& + 2 \operatorname{Im} (U_{e2} U_{\mu 2}^* U_{e3}^* U_{\mu 3}) \sin \left[\frac{t}{\hbar} \left\{ (k_3^2 \hbar^2 c^2 \right. \right. \\
& \left. \left. + m_3^2 c^4)^{\frac{1}{2}} - (k_2^2 \hbar^2 c^2 + m_2^2 c^4)^{\frac{1}{2}} \right\} \right]
\end{aligned} \tag{30}$$